Supporting Information: Figs S1-S12, Tables S1-S9, Methods S1

Fig. S1

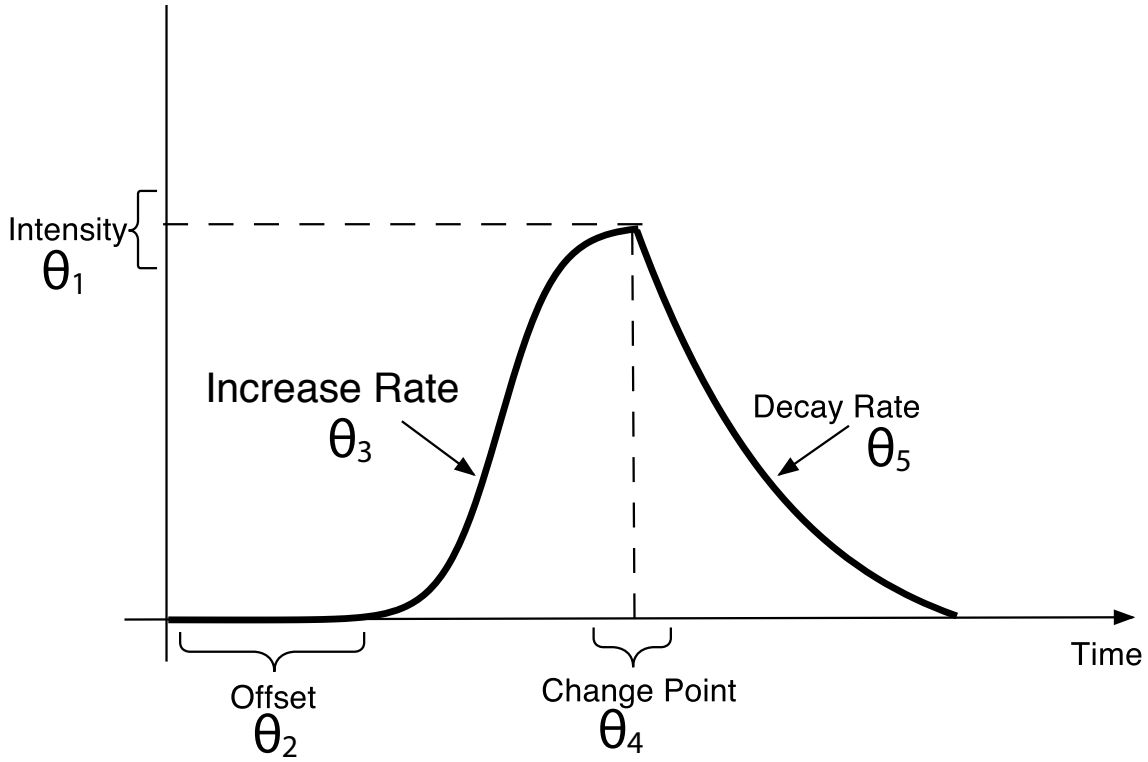

Fig. S1. Schematic of the 5 parameters analyzed for comparison of reactive oxygen species (ROS) generated by the various elicitors. See methods for more details.

Fig. S2

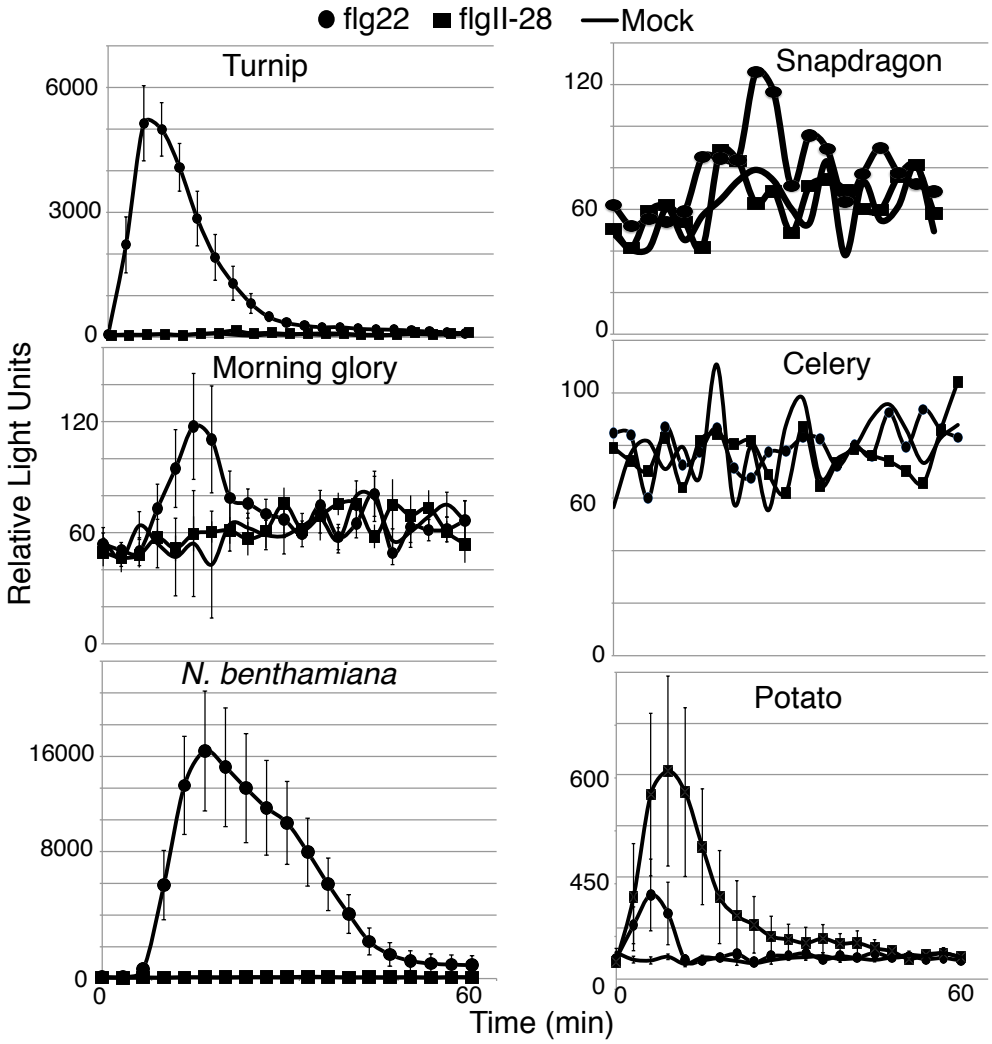

Fig. S2. Representative reactive oxygen species (ROS) curves from several data sets presented in Table 1. Leaf punches of Turnip cv. 'Purple Top White Globe', Snapdragon cv. 'Cook's Tall', Morning glory, Celery cv. 'S. V. Pascal', *N. benthamiana,* or Potato cv. 'Red Maria' were treated with 1μM of indicated peptides and then ROS was measured for 1 hour immediately following treatment. Data shown are the average of 6 replicate leaves and error bars represent standard error.

Fig. S3

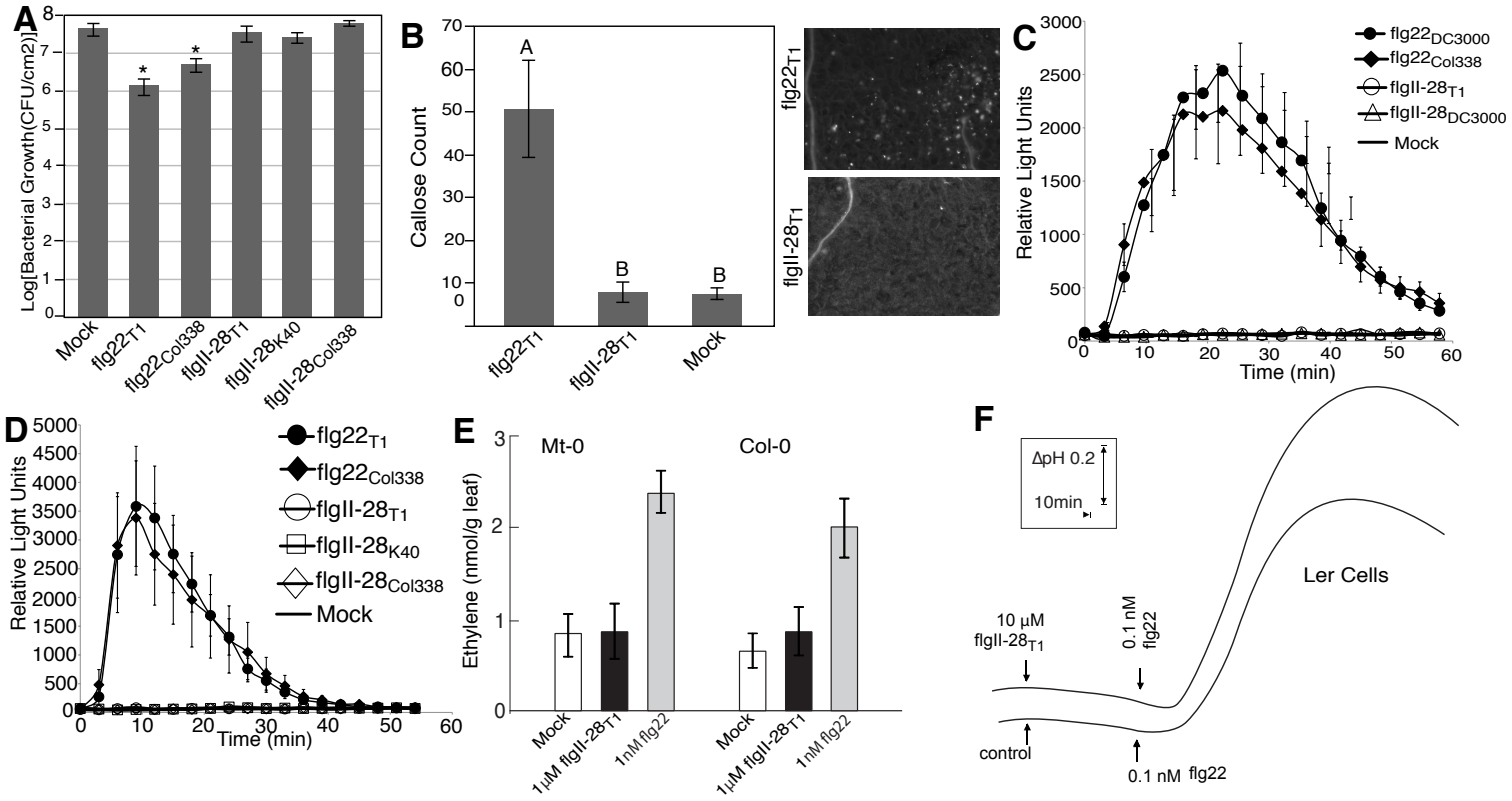

Fig. S3. Arabidopsis is blind to flgII-28 **A:** Leaves of *A. thaliana* eco. 'Col-0' were infiltrated with indicated peptides at 1 μM concentration. Strain DC3000 (was then spray infected onto the leaves 16 hours later and total bacterial populations were quantified 4 days following inoculation. Asterisks indicate significant differences in growth compared to mock treated plants in a pairwise comparison. Data shown are the average of 4 replicate leaves and error bars are the standard error. **B:** Leaves of *A. thaliana* ecotype 'Col-0' were infiltrated with 1μM flg22, flgII-28, or water (mock) and then stained for callose 22 hours later. Data shown represent the average amount of callose in 20 different fields of view from 4 separately infiltrated leaves and error bars are the standard error. **C&D:** Leaf punches of *A. thaliana* eco. 'Col-0' were treated with 1μM of indicated peptides and then reactive oxygen species (ROS) was measured for 1 hour immediately following treatment. Data shown are the average of 6 replicate leaves and error bars represent standard error. Similar results were obtained in at least 2 independent experiments for all sections. **E:** Leaf strips of 4 week-old *A. thaliana* eco. 'Col-0' or *A. thaliana* eco. 'Mt-0' were treated with the indicated peptides and ethylene production was measured after 4 hours of incubation following treatment. **F:** Alkalinization of extracellular pH in cell cultures derived *A. thaliana* eco. 'Ler' to treatment with flgII-28, flg22.

Fig. S4

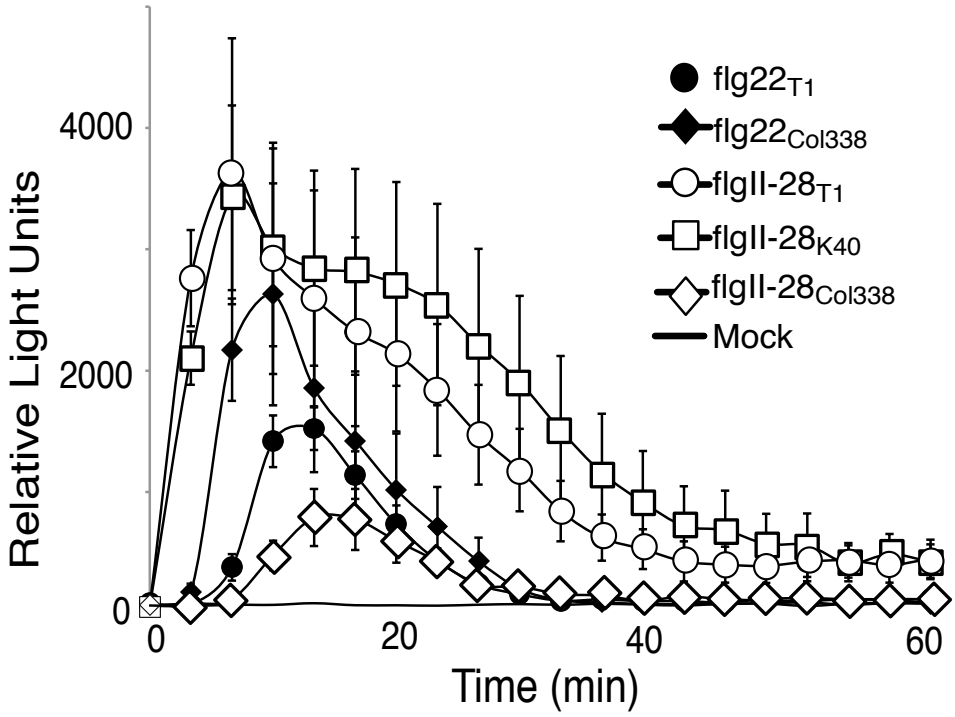

Fig. S4. Both flg22 and flgII-28 elicit production of reactive oxygen species (ROS) on tomato cv. 'Roter Gnom'. Leaf punches were treated with 1μM of indicated peptides and then ROS was measured for 1 hour immediately following treatment. Data shown are the average of 6 replicate leaves and error bars represent standard error. Similar results were obtained in 2 independent experiments.

Fig. S5

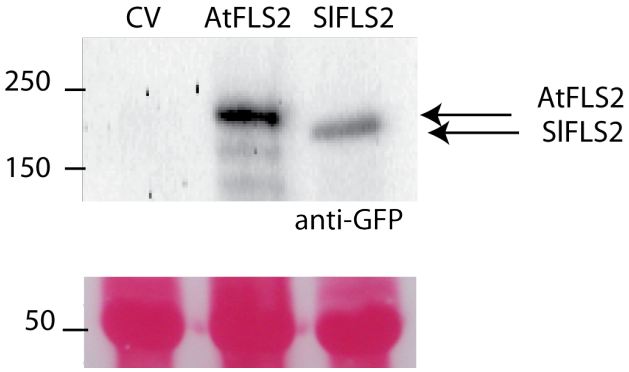

Fig. S5. Transient expression of *FLS2* led to stable heterologous expression of FLS2 proteins in *N. benthamiana*. Protein extracts were stained using anti-GFP antibody to detect the presence of the FLS2-GFP fusion proteins. The bottom panel shows a nonspecific band stained using Ponceau S as a loading control.

Fig. S6

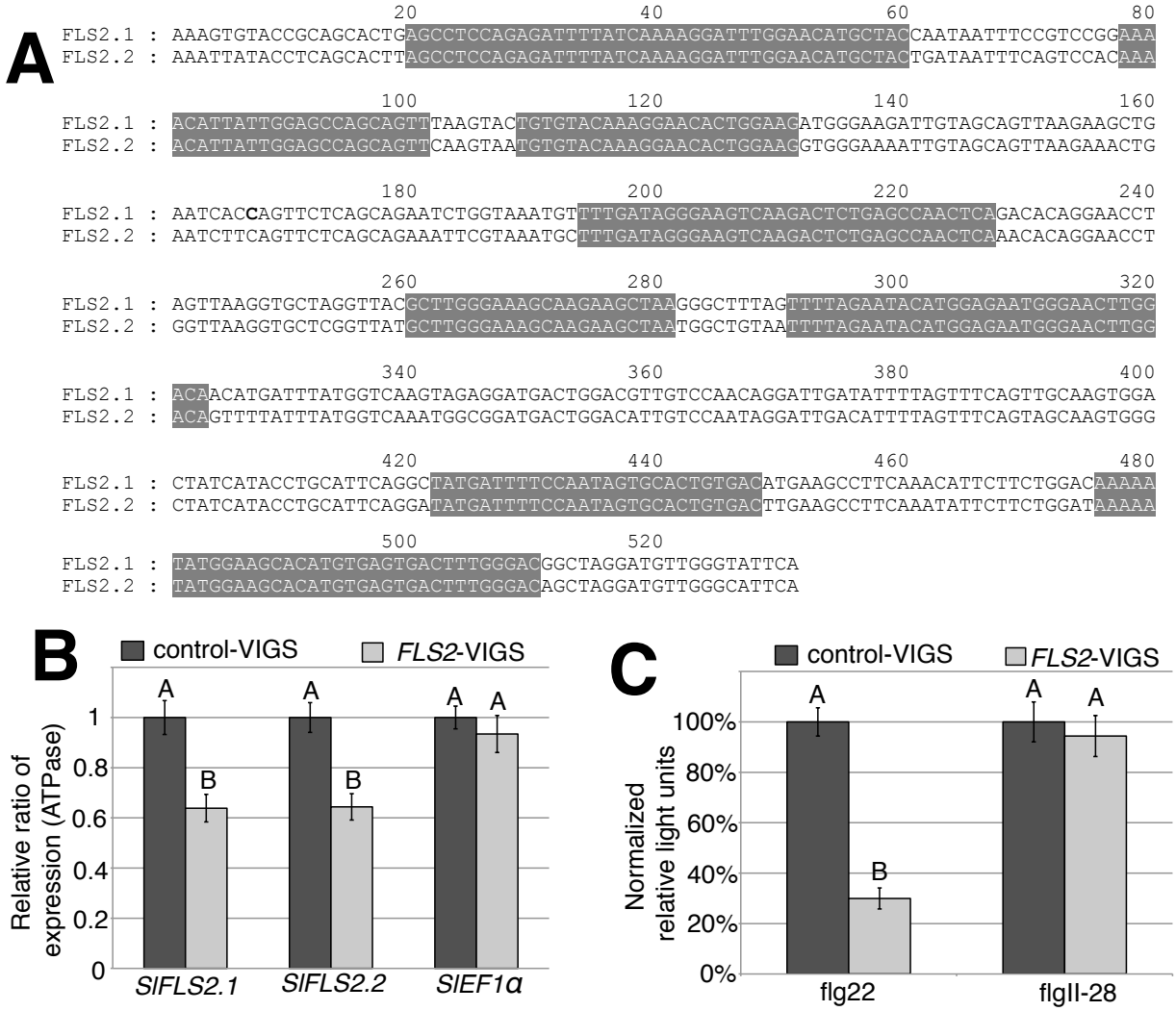

Fig. S6. (**A**) Comparison of similarity between the 531 bp fragment used for *FLS2* silencing (FLS2.1; Solyc02g070890) and the FLS2 paralog (FLS2.2; Solyc02g070910) in tomato. The grey boxes highlight regions with at least 21 contiguous identical nucleotides. (**B**) Transcript abundance of both *FLS2* genes was reduced in *FLS2*-VIGS tomato cv. 'Rio Grande' plants. Expression was analyzed by quantitative real time reverse transcription PCR (qRT-PCR) using *SlATPase* as a normalization control. Similar results were obtained using *SlEF1α* normalization. The relative ratio of expression sets 1.0 as the normalized expression of the gene in control-VIGS plants. Each bar represents the mean of 12 plants from 3 independent experiments and the bars show the standard error of the mean. (**C**) Total reactive oxygen species (ROS) production was calculated as described in Figure 4C using only plants tested in the qRT-PCR analysis in part B. Significant differences between control and *FLS2*-VIGS plants are indicated by different letters ($p < 0.001$).

Fig. S7

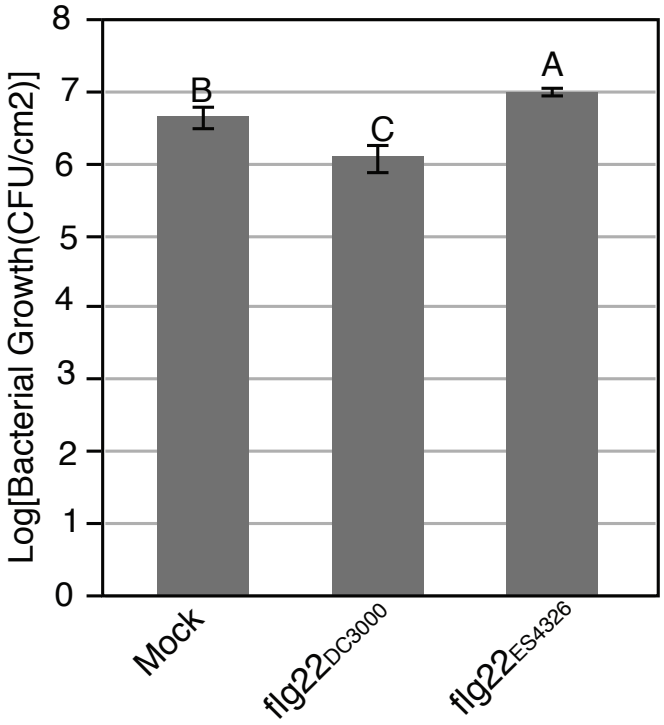

Fig. S7. Pretreatment with $flg22_{ES4326}$ leads to increased growth in a plant protection assay on tomato cv. 'Rio Grande'. Leaves of 4-week-old tomato were infiltrated with indicated peptides at 1μM concentration. Strain DC3000Δ*avrpto1*Δ*avrptoB* was then spray infected onto the leaves 16 hours later and total bacterial populations were quantified at 4 days. Different letters indicate significant differences at the 0.05 alpha level in an unpaired Student's t-test. Data represents the average of 4 replicate leaves. Similar results were obtained in 3 independent experiments.

Fig. S8

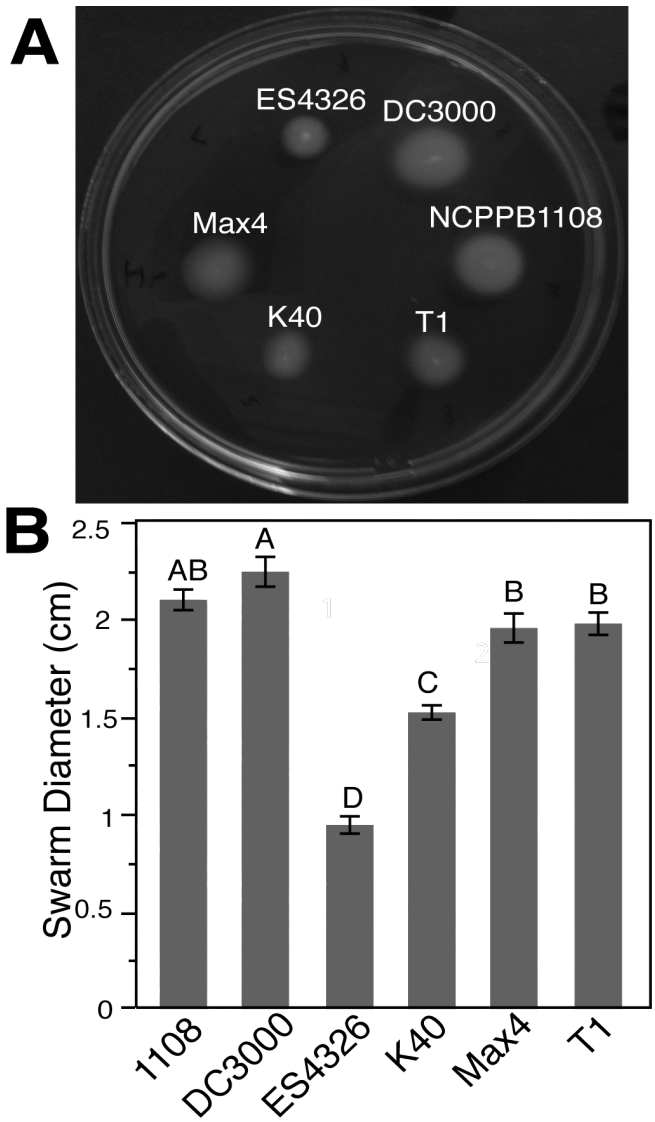

Fig. S8. Diversity in motility *in vitro* exists in the *P. syringae* species complex. **(A)** Representative picture of motility on a KB swim plate (0.3% agar) 2 days following toothpick inoculation with wild-type *P. syringae* strains. For quantification of motility in **(B)**, data represent the average of 8 replicate plates, error bars are the standard error, and letters indicate significant differences at the 0.05 alpha level in an unpaired Student's t-test. Similar results were obtained in 3 independent experiments.

Fig. S9

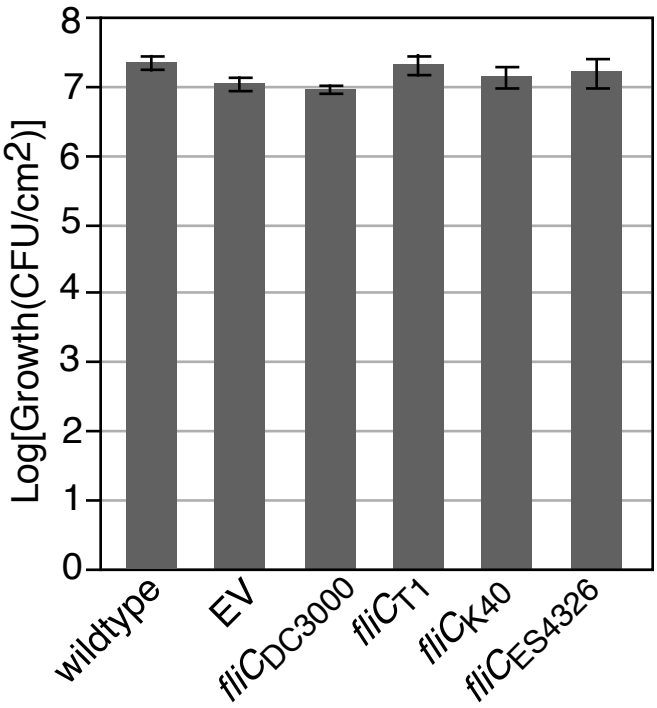

Fig. S9. The different alleles of *fliC* do not lead to varying growth on tomato before the onset of necrosis symptoms. 4 week-old tomato cv. 'Rio Grande' plants were syringe infiltrated with either wild-type DC3000 (wildtype), DC3000Δ*fliC* with an empty vector (EV) or DC3000Δ*fliC* complemented with the indicated alleles of *fliC* at $1x10^{-4}$ O.D. Growth was quantified 3 days following infection before the onset of necrosis symptoms. Similar results were obtained in 2 independent experiments. Data shown are the average of 4 replicate leaves and error bars represent standard error.

Fig. S10

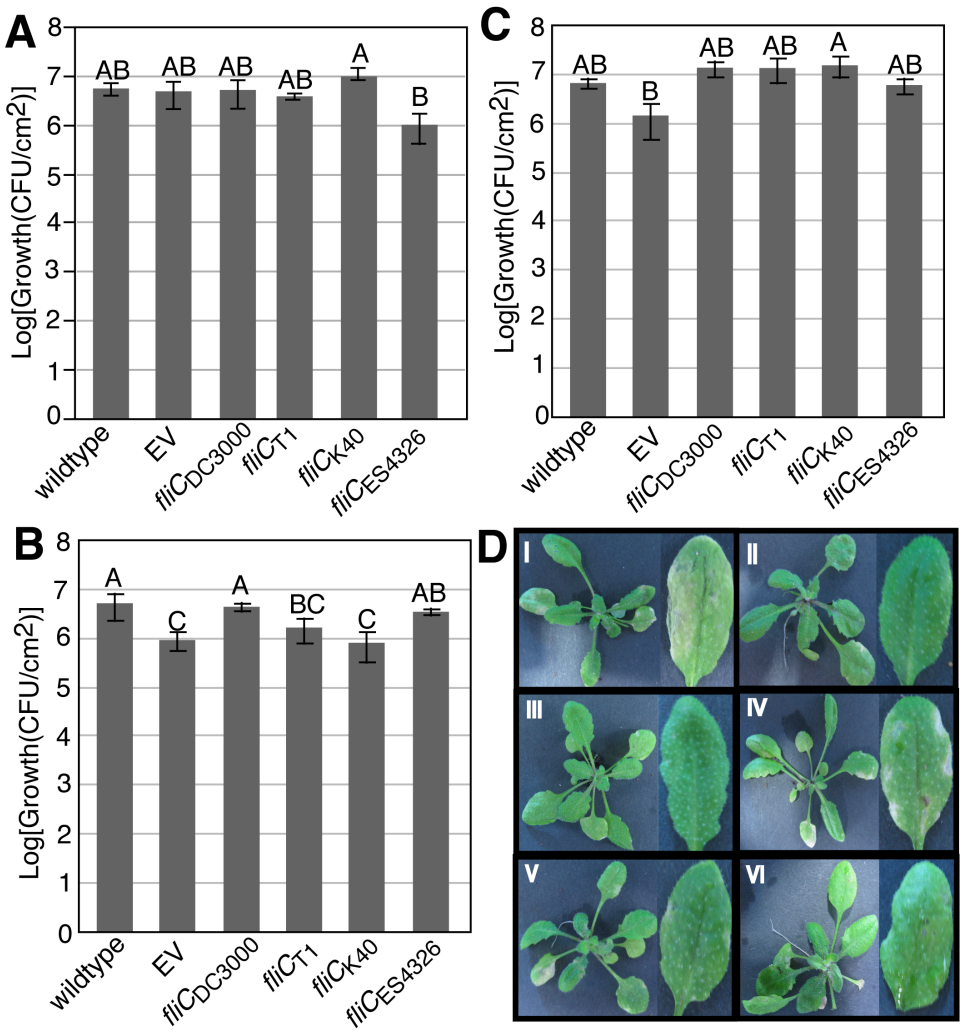

Fig. S10. Similar results as shown in Figures 7 and 8 (infiltration inoculation) are also observed following spray inoculation. Either wild-type DC3000 (wildtype), DC3000Δ*fliC* with an empty vector (EV) or DC3000Δ*fliC* complemented with the indicated alleles of *fliC* were spray inoculated at $1x10^{-2}$ O.D. onto either tomato cv. 'Rio Grande' (**A)**, *A. thaliana* eco. Col-0 (**B&D**), or *fls2* mutant *A. thaliana* eco. Col-0 (**C**). Growth was quantified 4 days following infection. For **D**, I is wildtype, II is $fliC_{K40}$, III is EV, IV is $fliC_{ES4326}$, V is $fliC_{T1}$, VI is $fliC_{DC3000}$. Data represent the average of 4 replicate leaves and error bars are standard error. Similar* results were obtained in at least 5 independent experiments.

*For **B,** DC3000Δ*fliC* complemented with $fliC_{K40}$ led to 3-15 fold lower growth than DC3000Δ*fliC* complemented with $fliC_{T1}$ in 13/15 experiments and 3-20 fold lower growth than DC3000Δ*fliC* complemented with $fliC_{DC3000}$ in 14/15 experiments but was not always a significant reduction in growth at our 0.05 alpha level cut off in a Student's t-test. DC3000Δ*fliC* complemented with $fliC_{T1}$ only had greater than 2 fold reduction in growth compared to DC3000Δ*fliC* complemented with $fliC_{T1}$ in 5/15 experiments and it was only significant at our cutoff in 2/15 experiments. On *fls2* plants, none of the alleles of *fliC* in the DC3000Δ*fliC* background led to any relative reduction in growth in any experiment.

Fig. S11

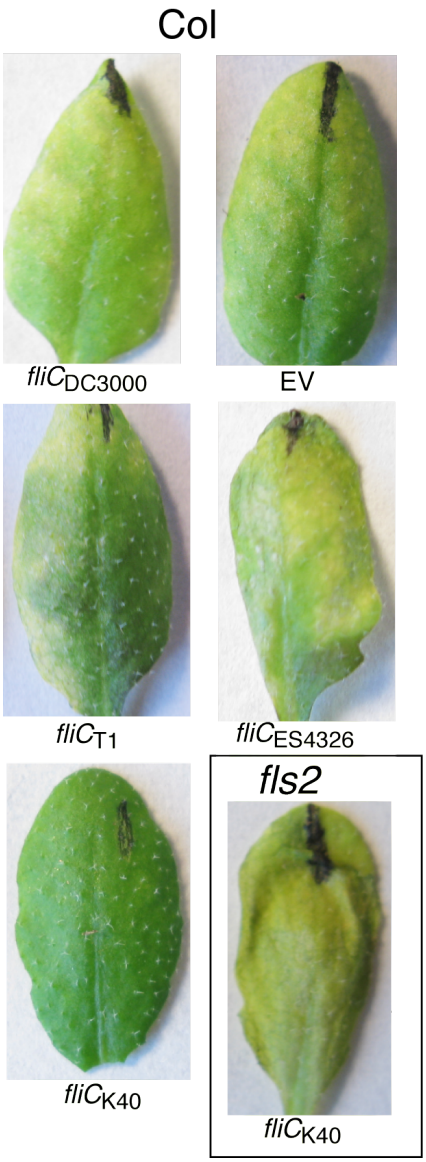

Fig. S11. Disease symptoms of *Arabidopsis* following infection with strains used in Figure 8. Representative pictures of disease symptoms on wild-type *Arabidopsis* (or *fls2* mutant in bottom right) following infiltration with either DC3000Δ*fliC* with an empty vector (EV) or DC3000Δ*fliC* complemented with the indicated alleles of *fliC* as in Figure 8.

Fig. S12

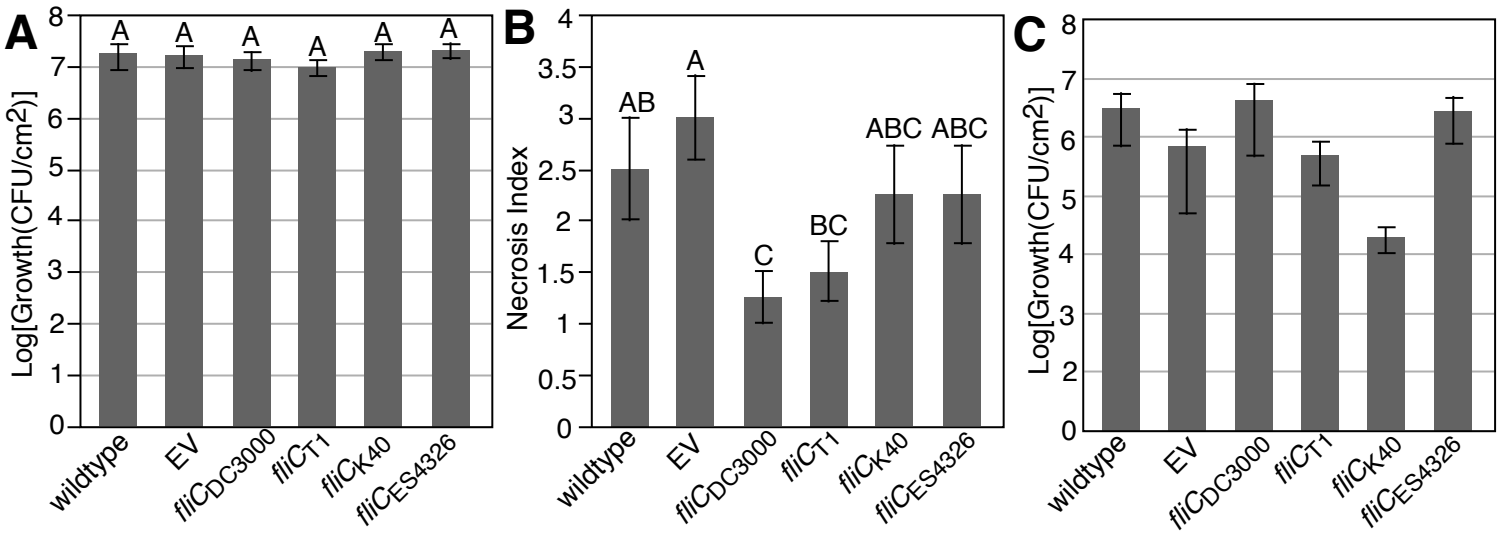

Fig. S12. Growth of second isolates of the DC3000Δ*fliC* strain complemented with the different alleles of *fliC*. **A&B:** Tomato cv. 'Rio Grande' plants were infiltrated at $1x10^{-4}$ O.D. with either wild-type DC3000 (wildtype), DC3000Δ*fliC* with an empty vector (EV) or DC3000Δ*fliC* complemented with the indicated alleles of flagellin. Growth (A) and severity of necrosis symptoms (B) were recorded 4 days following the infection. For the necrosis index: 1 = no necrosis in infiltrated area, 2 = moderate necrosis in infiltrated area, 3 = heavy necrosis in infiltrated area, 4 = complete necrosis in infiltrated area. **C:** Arabidopsis eco. Columbia strains were infiltrated at $1x10^{-3}$ O.D. with the same strains as in part A. Growth was quantified at 4 days following the infection. Error bars represent standard error. Similar results were obtained in 2 independent experiments.

Table S1

Gene	Purpose	Forward Primer	Reverse Primer
fliC-upstream	*fliC* deletion	cggaattcGCGTTCGACATTTCGCTGG	cgggatccCTCGTTGGTTTGGTACTAC
fliC-downstream	*fliC* deletion	cgggatccATCGGCATGAGTTTTAGCGG	cggaattcTTGCCAGCTGGGTGATACCT
$fliC_{Pto}$	*fliC* cloning	aaaaagagctcGCCCGTGGCTAGTTCATC	aaaaactcgagAAAAAGCGAGAGAGCGCTATTA
$fliC_{ES4326}$	*fliC* cloning	aaaaagagctcCGACAAAGCCCCACAAAA	aaaaactcgagAAAAAGCGAGAGAGCACTGTT
SlFLS2.1	VIGS construct	AAAGTGTACCGCAGCACTGAGCC	TGAATACCCAACATCCTAGCCG
SlFLS2.1	qRT-PCR	TTGCAGCACTTGGATCTG	AACTCCGTGTCATTCACTTT
SlFLS2.2	qRT-PCR	GATCATACTTGGGCCTGTTT	TCCTCCGAGTCTTTCACTT
SlATPase	qRT-PCR	TTGCTGAAGCCTTGGCTCTTTACG	ACCAGCGCGAGAAGAAAGGATGAT
SlEF1a	qRT-PCR	TCCAAAGATGGTCAGACCCGTGAA	ATACCTAGCCTTGGAGTACTTGGG

Table S1. Primers used in this study. Lowercase, underlined sequences are restriction enzyme sites.

Table S2

strain	flg22	flgII-28
cit7	TRLSSGLKINSAKDDAAGL**N**IA	ESTNILQRMRELAVQSRNDSNSATDRVA
pja	TRLSSGLKINSAKDDAAGL**N**IA	ESTNILQRMRELAVQSRNDSNSATDRVA
ppiR6	TRLSSGLKINSAKDDAAGL**N**IA	ESTNILQRMRELAVQSRNDSNSATDRVA
psy61	TRLSSGLKINSAKDDAAGL**N**IA	ESTNILQRMRELAVQSRNDSNSATDRVA
psyB728a	**G**RLSSGLKI**M**SSKDDAAGL**N**IA	ESTNILQRMRELAVQSRNDSNSATDRVA
ptt	TRLSSGLKINSAKDDAAGL**N**IA	ESTNILQRMRELAVQSRNDSNS**A**TDRVA
pac	TRLSSGLKINSAKDDAAGL**N**IA	ESTNILQRMRELAVQSRNDSNS**D**TDR**V**A
pae	TRLSSGLKINSAKDDAAGLQIA	ESTNILQRMRELAVQSRNDSNSSTDRDA
pan	TRLSSGLKINSAKDDAAGLQI**V**	ESTNILQRMRELAVQSRNDSNSSTDRDA
PgyR4	TRLSSGLKINSAKDDAAGLQIA	ESTNILQRMRELAVQSRNDSNSSTDRDA
pla107	TRLSSGLKINSAKDDAAG**M**QIA	ESTNILQRMRELAVQSRNDSNSSTDRDA
pmo	TRLSSG**S**KINSAKDDAAG**M**QIA	ESTNILQRMRELAVQSRNDSNSSTDRDA
pmp	TRLSSGLKINSAKDDAAGLQIA	ESTNILQRMRELAVQSRNDSNSSTDRDA
pph1448a	TRLSSGLKINSAKDDAAGLQIA	ESTNILQRMRELAVQSRNDSNSSTDRDA
psy642	TRLSSGLKINSAKDDAAGLQIA	ESTNILQRMRELAVQSRNDSNSSTDRDA
pta	TRLSSGLKINSAKDDAAGLQIA	ESTNILQRMRELAVQSRNDSNSSTDRDA
ptoT1	TRLSSGLKINSAKDDAAGLQIA	ESTNILQRMRELAVQSRNDSNSSTDRDA
pla106	TRLSSGLKINSAKDDAAGLQIA	ESTNILQRMRELAVQSRNDSNS**A**TDR**E**A
pmaF1	TRLSSGLKINSAKDDAAGLQIA	ESTNILQRMRELAVQSRNDSNS**A**TDR**E**A
pmaM3	TRLSSGLKINSAKDDAAGL**L**IA	ESTNILQRMRELAVQSRNDSNS**A**TDR**E**A
pmaM6	TRLSSGLKINSAKDDAAGLQIA	ESTNILQRMRELAVQSRNDSNS**A**TDR**E**A
ptoDC3000	TRLSSGLKINSAKDDAAGLQIA	ESTNILQRMRELAVQSRNDSNS**A**TDR**E**A
poryzae	**G**RLSSGLKI**M**SAKDDAAGL**N**IA	ESTNILQRMRELAVQSRNDSNS**ES**DR**T**A
ptoCol198	TRLSSGLKI**I**SAKDDAAGLQIA	ESTNILQRMREL**V**VQSRNDSNSSTDRDA
ptoK40	TRLSSGLKINSAKDDAAGLQIA	ESTNILQRMRELAVQ**F**RNDSNSSTDRDA
PcalES4326	**E**RLS**T**G**K**KIN**T**A**S**DDA**G**G**SVTQ**	ES**VS**ILQRMRELAVQSRNDSNSS**EG**RDA

Table S2. Alleles of flg22 and flgII-28 present in *P. syringae sensu lato* species complex. Within flg22 and flgII-28, the same color shading indicates identical alleles. Bolded, larger fonts indicate polymorphisms relative to the PtoT1 alleles of flg22 and flgII-28. Strains identified by pathovar only are the strains sequenced in (Baltrus et al., 2011).

Baltrus, D.A., Nishimura, M.T., Romanchuk, A., Chang, J.H., Mukhtar, M.S., Cherkis, K., Roach, J., Grant, S.R., Jones, C.D., and Dangl, J.L. (2011). Dynamic Evolution of Pathogenicity Revealed by Sequencing and Comparative Genomics of 19 *Pseudomonas syringae* Isolates. PLoS Pathog *7*, e1002132.

Table S3

flgII-28$_{T1}$ - flgII-28$_{K40}$	***S. lycopersicum* cv. Sunpride**	***S. lycopersicum* cv. Rio Grande**	***C. annuum* cv. Jalapeno Early**
ΔIntensity	2792.12[1029, 8969]	2801.54 [827, 8734]	254.15 [-523.5, 852.3]
ΔOffset	1.53[1.00, 1.96]	1.81[1.14, 2.18]	0.67 [-0.12, 1.67]
ΔIncrease Rate	6.67[-24.08, 37.67]	0.41[-34.31, 33.94]	-7.92 [-38.70, 27.72]
ΔChange Point	-2.81[-4.12, -1.51	-2.01[-3.80, -0.13]	1.01 [-3.55, 5.99]
ΔDecay Rate	-0.11[-0.24, 0.00]	-0.89 [-1.45, -0.07]	-0.13 [-0.25, 0.00]

Table S3. Difference in reactive oxygen species (ROS) response of *Solanaceae* plants shown in Figure 2 to either the T1 allele or the K40 allele of flgII-28. Non-bracketed numbers indicate the expected differential value for the five parameters described in Supplementary Figure 2 between flgII-28$_{T1}$ and flgII-28$_{K40}$. Positive values indicate that flgII-28$_{T1}$ had the higher peak intensity, shorter offset, higher increase rate, earlier change point, or higher decay rate. Numbers in bracket are the 95% Bayesian credible interval of the difference in value between flgII-28$_{T1}$ and flgII-28$_{K40}$. We consider the response difference between the two peptides significant if the 95% credible interval of the differential value does not overlap 0 (indicated by grey background highlighting). Similar results obtained at least 4 independent experiments.

Table S4

flgII-28$_{T1}$ - flgII-28$_{Col338}$	***S. lycopersicum* cv. Sunpride**	***S. lycopersicum* cv. Rio Grande**	***C. annuum* cv. Jalapeno Early**
ΔIntensity	5074.1 [3410, 11280]	3204.59 [1369, 9206]	-9.38 [-762.7, 556.7]
ΔOffset	1.45[0.86, 1.98]	0.49 [-0.18, 1.06]	0.22 [-0.66, 1.22]
ΔIncrease Rate	10.54[-18.72, 38.75]	-0.35 [-36.08, 35.71]	-0.57 [-35.57, 33.31]
ΔChange Point	-5.33[-7.38, -2.61]	-0.59 [-2.24, 1.28]	1.65 [-2.90, 6.57]
ΔDecay Rate	-44.1[-79.2, 0.01]	0.02[-0.07,0.09]	-0.05 [-0.13, 0.07]

Table S4. Difference in reactive oxygen species (ROS) response of *Solanaceae* plants shown in Figure 2 to either the T1 allele or theCol338 allele of flgII-28. Non-bracketed numbers indicate the expected differential value for the five parameters described in Supplementary Figure 2 between flgII-28$_{T1}$ and flgII-28$_{Col338}$. Positive values indicate that flgII-28$_{T1}$ had the higher peak intensity, shorter offset, higher increase rate, earlier change point, or higher decay rate. Numbers in bracket are the 95% Bayesian credible interval of the difference in value between flgII-28$_{T1}$ and flgII-28$_{Col338}$. We consider the response difference between the two peptides significant if the 95% credible interval of the differential value does not overlap 0 (indicated by grey background highlighting). Similar results obtained at least 4 independent experiments.

Table S5

flgII-28$_{T1}$ - flgII-28$_{K40}$	***S. lycopersicum* cv. Chico III**	***S. tuberosom* cv. Red Maria**	***C. annuum* cv. CA Wonder**
ΔIntensity	1003.28 [-1860.87, 3630.31]	607.28 [299.89, 1500.96]	1226.7 [-634.5, 12142.9]
ΔOffset	2.37 [1.51, 3.35]		-7.16 [-79.96, 2.50]
ΔIncrease Rate	-1.2 [-7.22, 5.14]		-5.41 [-39.15, 30.39]
ΔChange Point	-1.94 [-3.93, -0.10]		5.05 [0.93, 10.37]
ΔDecay Rate	-0.69 [-2.47, -0.12]		39.42 [2.88, 76.36]

Table S5. Difference in reactive oxygen species (ROS) response of other *Solanaceae* plants to either the T1 allele or the K40 allele of flgII-28. Non-bracketed numbers indicate the expected differential value for the five parameters described in Supplementary Figure 2 between flgII-28$_{T1}$ and flgII-28$_{K40}$. Positive values indicate that flgII-28$_{T1}$ had the higher peak intensity, shorter offset, higher increase rate, earlier change point, or higher decay rate. Numbers in bracket are the 95% Bayesian credible interval of the difference in value between flgII-28$_{T1}$ and flgII-28$_{K40}$. We consider the response difference between the two peptides significant if the 95% credible interval of the differential value does not overlap 0 (indicated by grey background highlighting). Similar results obtained at least 3 independent experiments. Black highlighting indicates that one peptide did not trigger any ROS and thus comparing parameters other than intensity is not meaningful.

Table S6

flgII-28$_{T1}$ - flgII-28$_{Col338}$	***S. lycopersicum* cv. Chico III**	***S. tuberosom* cv. Red Maria**	***C. annuum* cv. CA Wonder**
ΔIntensity	2129.97 [830.25, 4690.16]	578.05 [268.16, 1468.73]	1376.54 [-474.3, 12396.3]
ΔOffset	1.21 [0.46, 1.86]		-6.21 [-78.91, 3.55]
ΔIncrease Rate	0.17 [-6.55, 6.72]		-3.47 [-36.52, 31.26]
ΔChange Point	-0.34 [-2.33, 1.44]		2.94 [-1.51, 8.30]
ΔDecay Rate	-0.13 [-0.33, 0.02]		39.26 [2.84, 76.20]

Table S6. Difference in reactive oxygen species (ROS) response of other *Solanaceae* plants to either the T1 allele or theCol338 allele of flgII-28. Non-bracketed numbers indicate the expected differential value for the five parameters described in Supplementary Figure 2 between flgII-28$_{T1}$ and flgII-28$_{Col338}$. Positive values indicate that flgII-28$_{T1}$ had the higher peak intensity, shorter offset, higher increase rate, earlier change point, or higher decay rate. Numbers in bracket are the 95% Bayesian credible interval of the difference in value between flgII-28$_{T1}$ and flgII-28$_{Col338}$. We consider the response difference between the two peptides significant if the 95% credible interval of the differential value does not overlap 0 (indicated by grey background highlighting). Similar results obtained at least 3 independent experiments. Black highlighting indicates that one peptide did not trigger any ROS and thus comparing parameters other than intensity is not meaningful.

Table S7

flg22$_{T1}$ - flg22$_{Col338}$	***S. lycopersicum* cv. Sunpride**	***S. lycopersicum* cv. Rio Grande**	***C. annuum* cv. Jalapeno Early**
ΔIntensity	-1792.42 [-3911, -366.6]	709.17 [363, 1137]	-519.9 [-1767, 59.62]
ΔOffset	-0.32[-1.00, 0.09]	0.54 [0.10, .97]	-1.43 [-2.15, -0.49]
ΔIncrease Rate	-3.74[-35.91, 31.63]	-13.09[-41.24, 21.31]	3.20 [-31.69, 36.74]
ΔChange Point	0.72[-0.93, 2.58]	-1.87[-3.40, -0.80]	2.63 [0.23, 4.77]
ΔDecay Rate	0.17[-0.94, 0.62]	-2.49[-25.42, 0.06]	1.11 [0.04, 7.35

Table S7. Difference in reactive oxygen species (ROS) response of *Solanaceae* plants shown in Figure 2 to either the T1 allele or theCol338 allele of flg22. Non-bracketed numbers indicate the expected differential value for the five parameters described in Supplementary Figure 2 between flg22$_{T1}$ and flg22$_{Col338}$. Positive values indicate that flgII-28$_{T1}$ had the higher peak intensity, shorter offset, higher increase rate, earlier change point, or higher decay rate. Numbers in bracket are the 95% Bayesian credible interval of the difference in value between flg22$_{T1}$ and flg22$_{Col338}$. We consider the response difference between the two peptides significant if the 95% credible interval of the differential value does not overlap 0 (indicated by grey background highlighting). Similar results obtained at least 4 independent experiments for all plant-peptide combinations.

Table S8

$flg22_{T1}$ – $flg22_{col338}$	ΔIntensity	ΔOffset	ΔIncrease Rate	ΔChange Point	ΔDecay Rate
***S. lycopersicum* cv. Chico III**	-348.62 [-1165.53, 852.50]	-0.22 [-0.78, 0.12]	0.99 [-5.52, 6.82]	0.54 [-0.64, 1.74]	0.11 [-0.19, 0.48]
***S. tuberosom* cv. Red Maria**	295.23 [39.26, 880.58]				
***S. Melongena* cv. MM643**	-330.74[-781.0, 91.29]	0.14[-0.76, 0.91]	-7.06[-38.11, 29.17]	0.33[-2.78, 2.97]	30.97[-0.17, 67.43]
***C. annuum* cv. CA Wonder**	1421.53[-2566, 6101]	0.29[-0.22, .85]	-7.97[-39.09, 27.74]	0.13[-1.24, 1.41]	1.44[-0.17, 9.56]
N. benthamiana	3104.6[175.4, 5477.5]	1.16[.27, 1.96]	4.35[-25.97, 36.13]	-3.38[-5.84, -0.98]	-2.17[-12.64, 0.23]
***N. tabacum* cv. Burly**	8835.9[5556.9, 12132]	-0.79[-1.07, -0.28]	-0.39[-32.26, 33.41]	0.13[-0.86, 1.06]	-0.22[-0.62, 0.04]
Petunia X	-2683.6[-6567.96, 2007.09]	1.22 [0.14, 2.34]	-2.16 [-7.74, 3.03]	1.05 [-3.58, 4.88]	-0.10 [-0.22, 0.06]

Table S8. Difference in reactive oxygen species (ROS) response of other *Solanaceae* plants to either the T1 allele or theCol338 allele of flg22. Non-bracketed numbers indicate the expected differential value for the five parameters described in Supplementary Figure 2 between $flg22_{T1}$ and $flg22_{Col338}$. Positive values indicate that flgII-28_{T1} had the higher peak intensity, shorter offset, higher increase rate, earlier change point, or higher decay rate. Numbers in bracket are the 95% Bayesian credible interval of the difference in value between $flg22_{T1}$ and $flg22_{Col338}$. We consider the response difference between the two peptides significant if the 95% credible interval of the differential value does not overlap 0 (indicated by grey background highlighting). Similar results obtained at least 3 independent experiments. Black highlighting indicates that one peptide did not trigger any ROS and thus comparing parameters other than intensity is not meaningful. Similar results obtained in at least 3 independent experiments for all plant-peptide combinations.

Table S9

Arabidopsis		
Elicitor:	**Bayes Factor[a]**	**P(H_0|Data)[b]**
flg22$_{DC3000}$	0.0000	0.0000
flg22$_{ES4326}$	1956.4196	0.9995
Tomato		
Elicitor:	**Bayes Factor[a]**	**P(H_0|Data)[b]**
flg22$_{DC3000}$	0.0001	0.0001
flg22$_{ES4326}$	1872.0275	0.9995

Table S9. Analysis of the reactive oxygen species (ROS) response of either *A. thaliana* or tomato to either flg22$_{DC3000}$ or flg22$_{ES4326}$ shown in Figures 5A and 5B. [a]The Bayes Factor (H_0 vs Ha); [b]Probability of the null model (no response) explaining the observed data.

Methods S1

Reactive oxygen species (ROS) Curve Analysis

Explanation of model

ROS response consists of two phases: *growth* and decay. Isolating these two phases is critical to our analysis. While classical asymptotic methods could be employed to distinguish that the entire ROS reaction can be distinguished under varying conditions, we are interested in exactly how the reaction changes. That is, we wish to understand: 1) how both the growth and decay rates vary, 2) how the reaction intensities vary, 3) how long it takes for the reaction to start, and 4) how long the reactions are sustained. As a basis for our analysis, we model the curve using two types of curves: Gompertz (Winsor, 1932) (with a shift) and exponential decay. Gompertz curves have a long-standing history of modeling biological growth rates. Supplementary Figure 2 shows a rough schematic illustration of the growth/decay process.

Mathematically, the classical Gompertz curve is defined through the function:

Equation 1 $$y(t) = \theta_1 e^{\theta_2 e^{t\theta_3}},$$

where the parameters $\{\theta_1, \theta_2, \theta_3\}$ represent the curve intensity, offset, and growth rate respectively. While this functional parameterization is appealing for strictly mathematical reasons, fitting such functions to real data can be somewhat prohibitive due to the scaling effect of the offset parameter θ_2. Loosely speaking, under this parameterization the offset parameter must vary greatly to shift the curve even small amounts. Because of this, we adopt a new parameterization, which we refer to as the shifted-Gompertz curve, which is defined as:

Equation 2

$$y_G(t) = \theta_1 e^{-e^{\theta_3 (t+\theta_2)}}$$

Under this formulation, the offset parameter (again denoted as θ_2) acts as a linear shift parameter, so that small changes in θ_2 result in equally small changes in the offset. This modification to the standard Gompertz curve makes each parameter easily identifiable, and estimable.

For decay, we model the curve as exponentially decaying, which follows as:

Equation 3 $$y_D(t) = e^{-t\theta_5}.$$

Hence, up to some point in time (call this time θ_4), the curve has the form of $y_G(t)$, and after time θ_4 the curve takes on the form of $y_D(t)$. Formally, we write this as:

Equation 4 $$y(t, \Theta) = \delta(t \le \theta_4) y_G(t) + \delta(t > \theta_4) C(\Theta) y_D(t),$$

where $C(\Theta)$ is a function of all the parameters which connects the two curves so that the end of the growth process matches the value at the beginning of the decay process.

Curve fitting

Given a set of experimentally observed growth curves, we are able to fit Gompertz-decay curves to the data and measure precisely how the fitted parameter sets vary across experiments. Specifically, we let $d_{i,t}$ denote a data point along the i^{th} curve, at time *t*, and let $d_{i,t} \sim Normal(y(t,\Theta),\sigma)$. That is, we envision that the observed data is normally distributed, with a mean centered at the Gompertz-decay curve. While other error distributions can be easily incorporated, the standard normal assumption was well supported by our data.

For fitting such a model, and quantifying the uncertainty in the fit parameter values $\Theta = \{\theta_1,\theta_2,\theta_3,\theta_4,\theta_5\}$, we rely on Markov Chain Monte Carlo (MCMC) (Gelfand and Smith, 1990) (Chib and Greenberg, 1995) and adopt a Bayesian methodology.

Limitations of ROS curve comparisons

Because of the inherent variability in ROS responses due to biological differences among plants, we recommend only employing this approach to compare different peptides on *the same* plant. We cannot compare the absolute values from different plant species or even different plants. In fact, to account for variability between different plants of the same species we collected leaf punches from the same leaf multiple times to be treated with the different peptides.

Implementing this analysis

Please visit genome.ppws.vt.edu/ROS for the Matlab file for running the MCMC to estimate the modeling parameters for the shifted Gompertz-decay curve and the Matlab file for comparing the ROS kinetic parameters between two different peptides treated on the same plant. Also available is a short user manual and example file.

Callose deposition assay

Callose deposition was detected using the procedure described by Adam and Somerville (Adam and Somerville, 1996). Briefly: Leaves to be stained were incubated in alcoholic lactophenol first at room temperature for 15 minutes and then at 65^{o}C for 30 minutes. Leaves were then transferred to a fresh alcoholic lactophenol solution for 24 hours of further incubation at room temperature. The alcoholic lactophenol was subsequently replaced with first 50% ethanol and then distilled water to rinse the leaves. Analine blue (0.01% w/v) was used to stain the leaves for 30 minutes at room temperature. Callose was detected using the DAPI filter on a Zeiss Axio Imager.M1 microscope. For quantification, grayscale pictures of 5 separate leaf areas from 4 different leaves for each treatment group were collected. Individual image files were imported into ImageJ, the background was subtracted, the threshold for detection was adjusted to just eliminate the autofluorescence of vascular tissue, and the total area and number of particles was quantified using the analyze particles tool with threshold ranges of 10-infinity pixel^2 size and 0.1-1 circularity.

FLS2 protein detection

For detection of FLS2 proteins, *N. benthamiana* leaves (~80 mg powder) were frozen in liquid nitrogen and ~80 mg frozen tissue was homogenized in 50 µL of cold extraction buffer (Tris 50mM pH 7,5). Equal amount of proteins were separated by 8% SDS-PAGE and analyzed by Western blot with anti-GFP antibodies.

Quantitative real time reverse transcription PCR (qRT-PCR)

Total RNA was isolated using the RNeasy plant mini kit (Qiagen, Valencia, CA, USA). Four micrograms total RNA was treated with TURBO DNA-*free* kit (Life Technologies, Grand Island, NY, USA) twice for 30 minutes at 37°C with 1.5U DNase added before each incubation, and enzyme was removed using DNase Inactivation Reagent. After DNase treatment, 1.6µg RNA was used to prepare cDNA using SuperScript III First-Strand Synthesis System (Life Technologies) with oligo$(dT)_{20}$. Quantitative RT-PCR was performed using 200nM sequence-specific primers according to (Nguyen et al., 2010) with the cycling conditions according to (Zeng et al., 2012). The significance of the expression data was analyzed using a pairwise Student's *t* test ($P < 0.001$). Primer efficiencies were 1.9-2.0 for all primer pairs and primers sequences are given in Table S9.

Supporting References

Adam, L., and Somerville, S.C. (1996). Genetic characterization of five powdery mildew disease resistance loci in Arabidopsis thaliana. The Plant Journal *9*, 341-356.

Baltrus, D.A., Nishimura, M.T., Romanchuk, A., Chang, J.H., Mukhtar, M.S., Cherkis, K., Roach, J., Grant, S.R., Jones, C.D., and Dangl, J.L. (2011). Dynamic Evolution of Pathogenicity Revealed by Sequencing and Comparative Genomics of 19 *Pseudomonas syringae* Isolates. PLoS Pathog *7*, e1002132.

Chib, S., and Greenberg, E. (1995). Understanding the Metropolis-Hastings Algorithm. The American Statistician *49*, 327-335.

Gelfand, A.E., and Smith, A.F.M. (1990). Sampling-Based Approaches to Calculating Marginal Densities. Journal of the American Statistical Association *85*, 398-409.

Nguyen, H.P., Chakravarthy, S., Velasquez, A.C., McLane, H.L., Zeng, L., Nakayashiki, H., Park, D.-H., Collmer, A., and Martin, G.B. (2010). Methods to Study PAMP-Triggered Immunity Using Tomato and Nicotiana benthamiana. Molecular Plant-Microbe Interactions *23*, 991-999.

Winsor, C.P. (1932). The Gompertz Curve as a Growth Curve. Proceedings of the National Academy of Sciences of the United States of America *18*, 1-8.

Zeng, L., Velásquez, A.C., Munkvold, K.R., Zhang, J., and Martin, G.B. (2012). A tomato LysM receptor-like kinase promotes immunity and its kinase activity is inhibited by AvrPtoB. The Plant Journal *69*, 92-103.